

# ELECTRODEPOSITION AND CHARACTERIZATION OF Cu-Zn ALLOY FILMS OBTAINED FROM A SULFATE BATH

## ELEKTRONANOS IN KARAKTERIZACIJA PLASTI ZLITIN Cu-Zn, NASTALIH IZ SULFATNE KOPELI

**Abdelouahab Redjehta<sup>1</sup>, Kzmel Loucif<sup>1</sup>, Loubna Mentar<sup>2</sup>, Mohamed Redha Khelladi<sup>2</sup>,  
Abdelkrim Beniaiche<sup>3</sup>**

<sup>1</sup>Laboratoire des Matériaux Non Métalliques, Institut d'Optique et Mécanique de Précision, Université Ferhat Abbas-Sétif 1, 19000 Sétif, Algeria

<sup>2</sup>Laboratoire de Chimie, Ingénierie Moléculaire et Nanostructures, Ferhat Abbas-Sétif 1, 19000 Sétif, Algeria

<sup>3</sup>Laboratoire des Systèmes Photoniques et Optiques Non Linéaires, Institut d'Optique et Mécanique de Précision, Université Ferhat  
Abbas-Sétif 1, 19000 Sétif, Algeria  
redjehtaabdelouahab@yahoo.fr

*Prejem rokopisa – received: 2013-02-26; sprejem za objavo – accepted for publication: 2013-04-16*

In this work, we report the influence of the deposition potential on the electrodeposition process, current efficiency, surface morphology and microstructure of Cu-Zn alloys deposited on a Ru substrate from a sulfate solution with an addition of EDTA. The study was carried out by means of cyclic voltammetry (CV), chronoamperometry, atomic force microscopy (AFM) and X-ray diffraction (XRD) techniques analyzing the electrochemical behavior, surface morphology and structural characterization, respectively. The experimental results show that the electrochemical behavior of Cu-Zn electrodeposits varied with the deposition potential. The AFM measurement showed that the Cu-Zn thin films obtained at all the potentials are homogenous in appearance being of a small crystallite size, and a variation in the film roughness with deposition potentials is established. An analysis of X-ray diffraction patterns indicates that the electrodeposited Cu-Zn alloys exhibit  $\beta$ - and  $\gamma$ -phases.

Keywords: copper-zinc, electrodeposition, cyclic voltammetry, morphology, X-ray diffraction

V tem delu poročamo o vplivu potenciala nanosa pri postopku elektronanašanja na učinkovitost toka, morfologijo površine in mikrostrukturo zlitine Cu-Zn, nanosene na podlago iz Ru iz sulfatne raztopine z dodatkom EDTA. Za analizo elektrokemijskega vedenja, morfologije površine in značilnosti strukture so bile uporabljene ciklična voltametrij (CV), kronoamperometrija, mikroskopija na atomsko silo (AFM) in rentgenska difrakcija (XRD). Rezultati raziskav kažejo, da se elektrokemijsko vedenje elektronanosov Cu-Zn spreminja s spreminjanjem potenciala pri nanašanju. AFM-meritve so pokazale, da so tanke plasti Cu-Zn, dobljene pri vseh potencialih, na videz homogene z majhnimi kristalnimi zrnji, spreminjanje potenciala pa vpliva na hrapavost površine. XRD-analize kažejo, da zlitina Cu-Zn po elektronanosu vsebuje  $\beta$ - in  $\gamma$ -faze.

Ključne besede: baker-cink, elektronanos, ciklična voltametrij, morfologija, rentgenska difrakcija

## 1 INTRODUCTION

The production of the coatings made of zinc and its alloys has recently been of interest since alloy coatings provide a better corrosion protection than pure-zinc coatings. In addition, alloy coatings are very interesting due to their high strength, good plasticity and excellent mechanical properties. There are several methods for obtaining these alloys: physical vapor deposition (PVD), chemical vapor deposition (CVD), sputtering and molecular beam epitaxy (MBE) techniques are just a few of them. These methods have several advantages and are used for specific applications. However, due to certain limitations, such as high capital and high-energy costs, an alternative method is required. Recently, the electrochemical deposition (electrodeposition) has been used as an alternative technique for producing these structures on different surfaces. Electrochemical processes offer many advantages, including a room-temperature operation, low-energy requirements, fast deposition rates, a fairly uniform deposition over complex three-dimensional objects, low costs and a simple scale-up with an easily

maintainable equipment.<sup>1</sup> The control of the solution composition and deposition parameters determines the properties of a deposit. In electrodeposition, the mechanism growth, the morphology and the micro-structural properties of a film depend on electrodeposition conditions such as the electrolyte composition, the electrolyte pH and the deposition potential.<sup>2</sup>

Numerous studies of the electrodeposition of Cu-Zn alloys from aqueous baths have been carried out.<sup>3,4</sup> It has been reported that different electrochemical deposition parameters such as deposition potential or current density, temperature, pH, substrate-surface preparation and bath composition affect considerably the properties of deposits.<sup>5-9</sup> It is known that high-quality micrometer-thick films (smooth and bright deposits) can be prepared at a reasonably high deposition rate using baths with a high metallic-ion concentration and small amounts of additives.<sup>10,11</sup> In the same way, due to a large difference between the standard electrode potentials of Cu and Zn ( $\approx 1.1$  V), these ions should be complex in electrodeposition solutions to facilitate their codeposition. Therefore, in

this work, an organic additive of  $C_{10}H_{14}Na_2O_8, 2H_2O$ , called EDTA, was added to the sulfate bath.

The objective of the present work was to study the electrodeposition process and properties of the Cu-Zn alloys from a sulfate electrolyte with EDTA. The morphology and structure of the deposits were examined.

## 2 EXPERIMENTAL WORK

A deposition of Cu-Zn alloys was carried out in a bath of 0.14 M  $CuSO_4$  for Cu, 0.06 M  $ZnSO_4$  for Zn (Aldrich) with the  $Na_2SO_4$  support electrolyte, 0.5 M  $H_3BO_3$  (in order to control the pH of the solution and improve the quality of the deposit) and 0.35 M  $C_{10}H_{14}Na_2O_8, 2H_2O$  (EDTA) at  $pH \approx 4.2$  (Table 1). All the measurements were made at room temperature. Ethylenediaminetetra acetic acid, widely abbreviated as EDTA, was chosen as the complexing agent for a deposition of these alloys. Plating baths were prepared from the chemicals of analytical grade and bidistilled water, and the pH was adjusted with dilute sulfuric acid when needed. Before the electrodeposition, each solution was stirred with a nitrogen gas flow. The conventional electrochemical measurements were taken using a glass cell consisting of a three-electrode assembly that was connected to a VoltaLab 40 (PGZ301 and Volta Master 4) controlled by a personal computer. A platinum sheet was used as the counter electrode (anode) and the cathode (the Ru substrate) potentials were referred with respect to the saturated calomel electrode (SCE). The working electrode was an thick Ru layer approximately 200 nm deposited by sputtering onto each silicon wafer at a low temperature (150 °C) to get a better adherence. Before the electrodeposition, the substrates were first cleaned ultrasonically in acetone and ethanol and then also with distilled and deionized water. The Cu-Zn thin-film deposition onto the Ru surface (an area of 0.5 cm<sup>2</sup>) was studied by means of cyclic voltammetry (CV) and chronoamperometry (CA) techniques. The CV for all the solutions was initially carried out between -1.2 V and 0.2 V (SCE) at a scan rate of 20 mV s<sup>-1</sup>. The surface morphologies of the deposits were examined with atomic force microscopy (AFM). The roughness (the root-mean-square height deviation) of the samples was obtained directly from the AFM software (PicoScan 5.3 from Molecular Imaging). The crystalline structures of the deposits were identified with X-ray diffraction using a Philips diffractometer with a  $2\theta$  range 10–100° and Cu  $K_{\alpha}$  radiation ( $\lambda = 0.15406$  nm).

## 3 RESULTS AND DISCUSSIONS

### 3.1 Electrochemical study

Cyclic voltammetry was performed to understand the electrochemical behavior of the Cu(II) and Zn(II) species on the Ru electrode. Figure 1 shows the cyclic voltammograms of the Ru electrode recorded in different ion

**Table 1:** Bath composition and conditions for the Cu-Zn electrodeposition

**Tabela 1:** Sestava kopeli in razmere pri elektronanašnju Cu-Zn

Bath	$ZnSO_4, 7H_2O/M$	$CuSO_4, 5H_2O/M$	$Na_2SO_4 /M$	$H_3BO_3 /M$	EDTA /M
Zn	0.06		1	0.5	0.35
Cu		0.14	1	0.5	
Cu-Zn	0.06	0.14	1	0.5	0.35

solutions of Cu, Zn and Cu-Zn. In effect, Figure 1a shows a cyclic voltammogram of a solution containing 0.14 M  $CuSO_4$  with a cathodic scan limit of -0.8 V vs. SCE. Two sharp peaks are observed at -0.141 V and 0.072 V, corresponding to a reduction and a dissolution of Cu, respectively. In the Cu electrodeposition, the charge transfer step is fast and the growth rate is controlled with the rate of the Cu-ion mass transfer to the

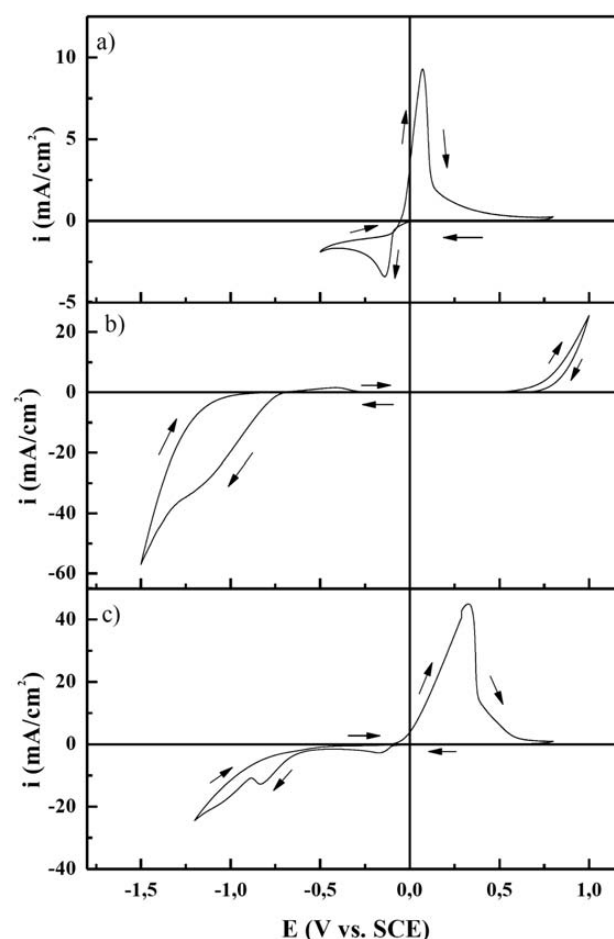


**Figure 1:** Cyclic voltammograms obtained for: a) 0.14 M  $CuSO_4$ , b) 0.06 M  $ZnSO_4$  + 0.35 M EDTA and c) 0.14 M  $CuSO_4$  + 0.06 M  $ZnSO_4$  + 0.35 M EDTA with the cathodic scan limit of -1.20 V vs. SCE, at the scan rate of 20 mV s<sup>-1</sup>; supporting electrolyte is 1 M  $Na_2SO_4$  + 0.5 M  $H_3BO_3$  (pH 4.2)

**Slika 1:** Ciklični voltamogrami, dobljeni z: a) 0,14 M  $CuSO_4$ , b) 0,06 M  $ZnSO_4$  + 0,35 M EDTA in c) 0,14 M  $CuSO_4$  + 0,06 M  $ZnSO_4$  + 0,35 M EDTA s katodno omejitvijo -1,20 V proti SCE, pri hitrosti skeniranja 20 mV s<sup>-1</sup>; osnovni elektrolit je 1 M  $Na_2SO_4$  + 0,5 M  $H_3BO_3$  (pH 4,2)

growing centers. The consistency of the cyclic-voltammetry behavior upon the potential cycling indicates that the anodic stripping process completely removes Cu from the electrode surface. The data in this figure indicates the absence of an underpotential deposition peak, with the Cu reduction occurring at the significant overpotential to the Nernstian value. This is due to a weak deposit/substrate interaction, as the early stages of an electrodeposition of Cu on Ru surfaces correspond to the Volmer-Weber growth mechanism.<sup>12</sup>

**Figure 1b** shows a cyclic voltammogram obtained in 0.06 M ZnSO<sub>4</sub>. During a direct scan, it is possible to note that the increase in the current begins at -0.7 V; this is due to the electrodeposition of Zn and hydrogen evolution. In the reverse potential scan, the absence of the peak corresponding to the dissolution of the previously deposited Zn is observed. For the Cu and Zn solution (**Figure 1c**), the voltammogram obtained shows the presence of cathodic and anodic peaks related to the deposition and dissolution of the metals. In the cathodic scan, it can be observed that the increases in the current were detected at -0.152 V and -0.75 V, being characteristic of the potential deposition processes of Cu and Zn onto Ru surfaces, respectively. After this limit, the hydrogen evolution is predominant. During the inverse of the potential scan, it is possible to observe, in all the curves, the presence of crossovers which are typical of the formation of a new phase involving a nucleation process.<sup>13</sup>

To elucidate the role of an applied potential, the current efficiency (CE) during the codeposition process was determined. The deposition CE was calculated from the ratio of the cathodic electric charge, which passed during the electrodeposition of the Cu-Zn alloy, to that of the anodic one required for the total alloy dissolution. The Cu-Zn alloy thin films were obtained in the potentiostatic mode at different deposition potentials. The dependence of CE on different deposition potentials is

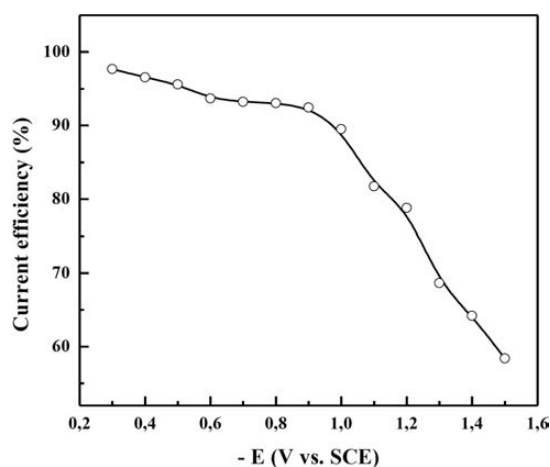


**Figure 2:** Effect of the deposition potential on the current efficiency of the Cu-Zn electrodeposition process

**Slika 2:** Vpliv potenciala nanosa na učinkovitost elektronanašanja Cu-Zn

shown in **Figure 2**. The efficiencies of the deposits decrease considerably with the potential and then reach their minima at more negative potentials. This decrease in CE is due to the process of hydrogen evolution. It is clear from these results that there is an appreciable decrease in the value of CE as the deposition potentials become more negative than  $\approx -1.0$  V. This is due to the hydrogen evolution reaction (HER) that becomes more significant than the Zn and Cu electrodeposition. This, in turn, increases the pH level at the cathode, causing the metal hydroxide to be included in the deposit.<sup>11</sup> These observations indicate that the control of the deposition potential is very important for realizing a high CE in the Cu-Zn deposition process. Similar results for Cu-Zn deposits are observed by de Almeida et al.<sup>14</sup>

The current was recorded as a function of time to study the deposition mechanisms of Cu-Zn alloys during their growth. The electrochemical deposition was performed using the standard chronoamperometry technique to study the nucleation and growth mechanism of Cu-Zn on ruthenium. Deposition potentials were chosen according to the reduction peaks appearing on the cyclic voltammograms. Deposition is conducted at the constant potentials in the potentiostatic mode, during which current transients are recorded. **Figure 3** shows the current transients obtained at four different potentials: -1.0 V, -1.1 V, -1.2 V and -1.3 V vs. SCE. In this figure, at the beginning of the applied potentials, a high cathodic current is seen for a short time. After that, the current rapidly decreases due to a depletion of the metal-ion concentrations close to the electrode surface, subsequently reaching a stable value. The current-time transients have a normal dependence on the overpotentials, whereas the current density increases with an increase in the overpotential. This is specific to the nucleation and growth process and for longer times, merging into a common curve caused by the diffusion-controlled pro-

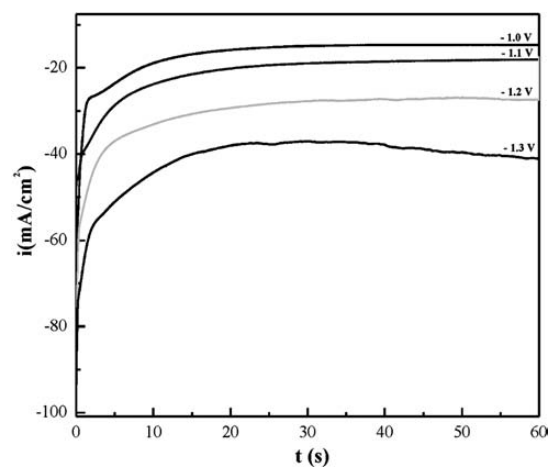


**Figure 3:** Evolution of current densities versus deposition time during the deposition of Cu-Zn on the Ru surface at different deposition potentials

**Slika 3:** Razvoj gostote toka v primerjavi s časom nanosa Cu-Zn na površino Ru pri različnih potencialih nanašanja

cess and described with the Cottrell equation.<sup>15</sup> According to the  $i-t$  curves, each transient has one well-defined, recognizable current maximum seen as a clear first peak followed by a sharp fall and subsequent growth. The  $i-t$  transients have a normal dependence on the overpotentials, whereas the current density increases with an increase in the overpotential. The peak corresponds to the nucleation of the metallic sites on the surface and it is followed by a reduction in the current exhibiting a three-dimensional (3D) growth. An increase in the peak current at higher overpotentials means that the number of sites (nucleation rate) increases due to a higher nucleation rate.<sup>15</sup>

### 3.2 Morphological and Structural Analysis

The morphology of the electrodeposited surface was imaged *ex situ* after the Cu-Zn electrodeposition using AFM measurements. **Figure 4** shows  $2\ \mu\text{m} \times 2\ \mu\text{m}$  AFM

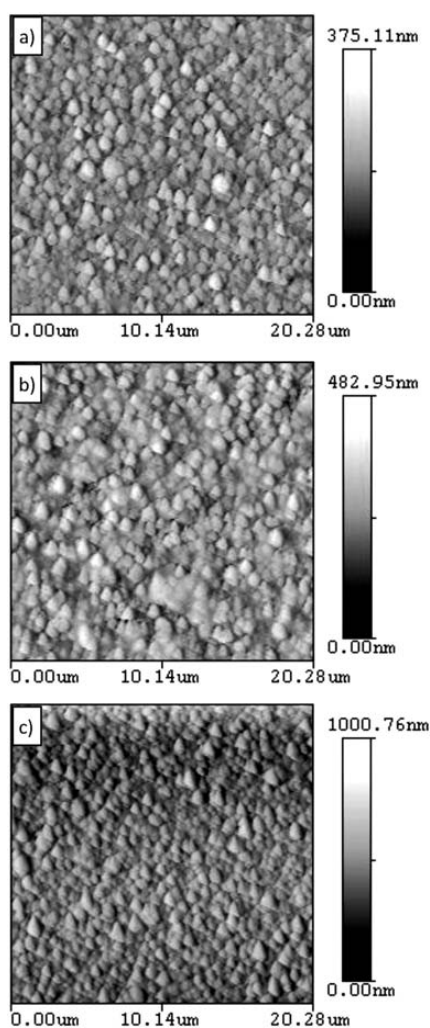


**Figure 4:** AFM images of the Cu-Zn thin films prepared at different cathodic potentials: a)  $-1.1\ \text{V}$ , b)  $-1.2\ \text{V}$  and c)  $-1.3\ \text{V}$  vs. SCE

**Slika 4:** AFM-posnetki tankih plasti Cu-Zn, pripravljenih pri različnih katodnih potencialih: a)  $-1,1\ \text{V}$ , b)  $-1,2\ \text{V}$  in c)  $-1,3\ \text{V}$  v odvisnosti od SCE

images of the deposited Cu-Zn alloy films obtained at different deposition potentials. The figures reveal that, with all the applied potentials, the images have a granular surface. However, the dimensions of the visible features in the images are different. It is known that a film electrodeposited on a polycrystalline substrate is also polycrystalline. During electrolysis, Cu-Zn crystallites randomly grow on the polycrystalline substrate and may form conglomerates. The composition and crystallite sizes strongly depend on the applied potential. If the current density is very small, there will be insufficient crystalline growth centers and the deposited layer will be rough-grained. If the current density is high, the deposited layer will be porous and soft.

The surface topography is traditionally analyzed with surface-roughness measurements such as the root-mean-square (RMS) roughness, the average roughness and the peak-to-valley roughness.<sup>16</sup> In brief, the surface roughness  $R_q$  (denoted also as RMS) and the mean roughness  $R_a$  were calculated using the standard software (**Table 2**). The surface roughness increases with the film thickness for the films deposited using both potentials, and the variation in the surface morphology with the applied potential is consistent with the general theory.<sup>17</sup>

**Table 2:** Dependence of the surface roughness and crystallite size of the electrodeposited Cu-Zn thin films on deposition potentials

**Tabela 2:** Odvisnost hrapavosti površine in velikosti kristalnih zrn Cu-Zn tanke plasti po elektronanašanju od potenciala pri nanosu

$E/(\text{V vs. SCE})$	$R_q/\text{nm}$	$R_a/\text{nm}$	$D/\text{nm}$
$-1.10$	42.72	33.12	48.20
$-1.20$	53.04	65.60	46.50
$-1.30$	108.62	82.08	46.10

The effect of the current density on this surface morphology can be explained since a high current density results in higher rates of the crystal nucleation (a higher mobility of atoms), giving rise to finer crystal structures and, hence, a smoother surface.<sup>17</sup> However, a new theory<sup>18,19</sup> has emerged, proposing that the concentration of metallic ions does change the bath homogeneously, but rather preferentially increases near the substrate (cathode). This relative concentration in the discharging zone is of a little significance at a low current density, at which the surface of a deposited film is rough. At a high current density, the convexity of the film increases, being associated with a relative concentration of ions in the discharging zone. The surface of a film deposited under these conditions is very smooth. The convex part of the film attracts more ions by acting as a focus of discharge, further increasing the convexity of the film. This may explain the mechanism of deposition.<sup>20</sup>

**Figure 5** shows the XRD patterns of the Cu-Zn films deposited on the Ru substrates in the sulfate/EDTA bath under different deposition potentials of  $-1.1\ \text{V}$ ,  $-1.2\ \text{V}$  and  $-1.3\ \text{V}$  vs. SCE in the  $2\theta$  scan range of  $25-60^\circ$ . All the XRD patterns show many peaks corresponding to two distinct phases,  $\beta$  and  $\gamma$ , respectively. It is clear that

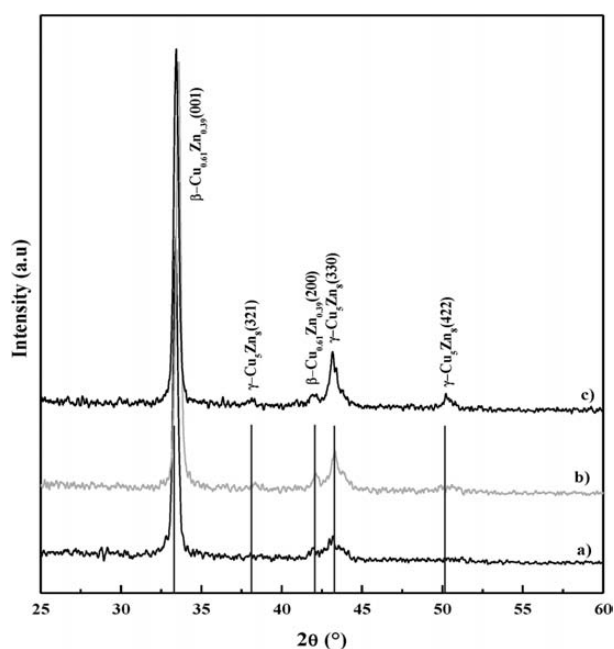


**Figure 5:** X-ray diffraction patterns of the electrodeposited Cu-Zn alloy films obtained at different deposition potentials: a)  $-1.1$  V, b)  $-1.2$  V and c)  $-1.3$  V vs. SCE

**Slika 5:** XRD-posnetki tankih plasti Cu-Zn, dobljeni pri različnih potencialih nanašanja: a)  $-1,1$  V, b)  $-1,2$  V in c)  $-1,3$  V v primerjavi s SCE

the XRD patterns from the Cu-Zn electrodeposits are different from those of pure Zn and Cu, indicating that crystalline alloys are indeed formed in these Cu-Zn electrodeposits. Furthermore, the  $\gamma$  phase diffraction lines increase in intensity as the deposition potential becomes more negative; in other words, the  $\gamma$  phase increases as the Cu content in the electrodeposited Cu-Zn alloy decreases. At a higher deposition potential, a decrease in the Cu concentration is explained with the fact that, at these potentials, a reduction in Cu is mass-transport limited. A further increase in the deposition overpotential would only increase the amount of Zn being deposited.<sup>21–23</sup> From these results, the  $\gamma$  phase was more dominant than the  $\beta$  phase in the Cu-Zn alloy thin films.

The average crystallite size of the particles is calculated from the full width at half maximum (FWHM) of the respective peaks using the Scherrer relation:<sup>24</sup>

$$D = \frac{0.9\lambda}{\beta \cos \theta} \quad (1)$$

where  $D$  is the crystallite size,  $\lambda$  is the wavelength of X-ray radiation ( $\lambda = 0.15406$  nm),  $\beta$  is the FWHM of the peak and  $\theta$  is the diffraction angle.

Also, **Table 2** shows the average crystallite size obtained from XRD for [001] planes, for the  $\beta$  phase of the alloys electrodeposited at three different applied potentials. The average crystallite size decreases with the increasing Zn concentration in the films and with the increasing applied potentials. This observation shows

that, at a more negative potential, the deposition rate is high and, hence, the atoms are incorporated in the film with little surface migration, thus limiting the grain size.

## 4 CONCLUSIONS

Smooth, compact and bright binary Cu-Zn alloys were deposited on a Ru substrate from a sulfate electrolyte with an EDTA additive. The electrodeposition behavior of the sulfate electrolyte was studied using cyclic voltammetry. A possibility of depositing pure copper and zinc with a trace of copper was revealed during a cathodic scan of the substrate potential. The effects of deposition potentials on the microstructures of Cu-Zn were investigated by means of AFM and XRD techniques. The AFM images showed Cu-Zn clusters of an equivalent size randomly distributed in the surface defects acting as active sites. An X-ray diffraction measurement reveals that the Cu-Zn alloy exhibits two phases, the  $\beta$  and  $\gamma$  phases. According to these results, the  $\gamma$  phase was more dominant than the  $\beta$  phase in the Cu-Zn alloy thin films.

## 5 REFERENCES

- D. Y. Park, N. V. Myung, M. Schwartz, K. Nobe, *Electrochim. Acta*, 47 (2002), 2893
- Southampton Electrochemistry Group, In: T. J. Kemp (Ed.), *Instrumental Methods in Electrochemistry*, Ellis Horwood Ltd., Chichester, UK 1985
- D. Pletcher, *Industrial Electrochemistry*, Chapman and Hall, London 1984, 187
- R. W. Mackey, In: F. A. Lowenheim (Ed.), *Modern Electroplating*, John Wiley & Sons, Inc., New York 1974, 418
- K. Raeissi, A. Saatchi, M. A. Golozar, J. A. Szpunar, *J. Appl. Electrochem.*, 34 (2004), 1249
- L. H. Mendoza-Huizar, C. H. Rios-Reyes, M. G. Gómez-Villegas, *J. Mex. Chem. Soc.*, 53 (2009), 243
- N. M. Younan, *J. Appl. Electrochem.*, 30 (2000), 55
- J. P. Millet, M. Gravria, H. Mazille, D. Marchandise, J. M. Cuntz, *Surf. Coat. Technol.*, 123 (2000), 164
- C. S. Lin, H. B. Lee, S. H. Hsieh, *Metall. Trans. A*, 31A (2000), 475
- P. F. J. de Leon, E. Albano, V. R. C. Salvarezza, *Phys Rev E*, 66 (2002), 1
- M. Paunovic, M. Schlesinger, *Fundamental of Electrochemical Deposition*, John Wiley & Sons, Inc., New Jersey, USA 2006, 210–218
- L. Huang, F. Z. Yang, S. K. Xu, S. M. Zhou, *Trans. Inst. Met. Finish*, 84 (2004), 47
- R. Greef, R. Peat, L. M. Peter, D. Pletcher, J. Robinson, *Instrumental Methods in Electrochemistry*, Ellis Horwood, Chichester 1985, Ch. 9
- M. R. H. de Almeida, E. P. Barbano, M. F. de Carvalho, I. A. Carlos, J. L. P. Siqueira, L. L. Barbosa, *Surface & Coatings Technology*, 206 (2011), 95
- A. J. Bard, L. R. Faulkner, *Electrochemical Methods, Fundamentals and Applications*, 2nd Ed., Wiley, New York 2001
- J. M. Bennett, L. Mattsson, *Introduction to Surface Roughness and Scattering*, Optical Society of America, Washington, D.C. 1989
- I. Ohno, *J. Surf. Finishing Soc. Jpn.*, 39 (1988), 149
- T. Watanabe, *The Surface Science Society of Japan, 2nd Thin Film Fundamental Seminar*, 1999, 115
- K. Inoue, T. Nakata, T. Watanabe, *Mater. Transact.*, 43 (2002), 1318

- <sup>20</sup> A. Sahari, A. Azizi, N. Fenineche, G. Schmerber, A. Dinia, Surf. Rev. Lett., 12 (2005), 391
- <sup>21</sup> M. R. Khelladi, L. Mentar, A. Azizi, L. Makhloufi, G. Schmerber, A. Dinia, J Mater Sci: Mater Electron, 23 (2012), 2245
- <sup>22</sup> L. Mentar, M. R. Khelladi, A. Beniaiche, A. Azizi, Int. J. Nanoscience, 12 (2013), 1250038
- <sup>23</sup> P. Y. Chen, M. C. Lin, I. W. Sun, J. Electrochem. Soc., 147 (2000), 3350
- <sup>24</sup> B. D. Cullity, Elements of X-ray Diffraction, Addison-Wesley, USA 1978